OFFICE OF NAVAL RESEARCH

PUBLICATIONS/PATENTS/PRESENTATIONS/HONORS REPORT

for

October 1, 1990 through September 30, 1991

for

Contract N00014-87-K-0243

R&T #414e340

Materials Processing of Diamond: Etching, Doping by Ion Implantation and Contact Formation

Max L. Swanson
University of North Carolina
Department of Physics and Astronomy
CB#3255 Phillips Hall
Chapel Hill, NC 27599-3255

a. Papers submitted and not yet published

1. "Methods of Creating Semiconducting Diamond", M.L. Swanson, H.D. Hunn and N.R. Parikh, Intern. Symp. on High Tech Materials, Nagoya, Nov. 5-8, 1991.

b. Papers published and accepted for publication

1. "Regrowth of Radiation-Damaged Layers in Natural Diamond", B. Liu, G.S. Sandhu, N.R. Parikh and M.L. Swanson, Nucl. Instr. Meth. B45, 420 (1990).

2. "Neutron Depth Profiling By Coincidence Spectrometry", N.R. Parikh, E.C. Frey, H.C. Hofsäss, M.L. Swanson, R.G. Downing, T.Z. Hossain, and W.K. Chu Nucl. Instr. Meth. B45, 70 (1990).

3. "Regrowth of Damaged Layers in Diamond Produced by Ion Implantation", G.S. Sandhu, B. Liu, N.R. Parikh , J.D. Hunn, M.L. Swanson, Th. Wichert, M. Deicher, H. Skudlik, W.N. Lennard, and I.V. Mitchell Mat. Res. Soc. Symp. Proc. 162, 189 (1990).

4. "Doping of Diamond by Co-Implantation with Dopant Atoms and Carbon", G.S. Sandhu, C.T. Kao, M.L. Swanson, and W.K. Chu, Mat. Res. Soc. Symp. Proc. 162, 321 (1990).

5. "Annealing of Implantation Damage in Single Crystal Diamond" , J.D. Hunn, M.L. Swanson, E.A. Hill, N.R. Parikh, and G. Hudson, in "New Diamond Science and Technology", eds. R. Messier et al. (MRS, Pittsburgh, 1991), p.929.

c. Books submitted for publication
none

d. Books published
none

e. Patent filed
none

f. Patents granted
W.K. Chu and C.B. Childs, July 20, 1989, "Coated Substrates and Process."

g. Invited presentations

M.L. Swanson, H.D. Hunn and N.R. Parikh, "Methods of Creating Semiconducting Diamond", Intern. Symp. on High Tech Materials, Nagoya, Nov. 5-8, 1991.

h. Contributed presentations
none

i. Honors, awards, prizes

j. Graduate students and post-doctorals supported

Graduate students: J.D. Hunn, E.A. Hill

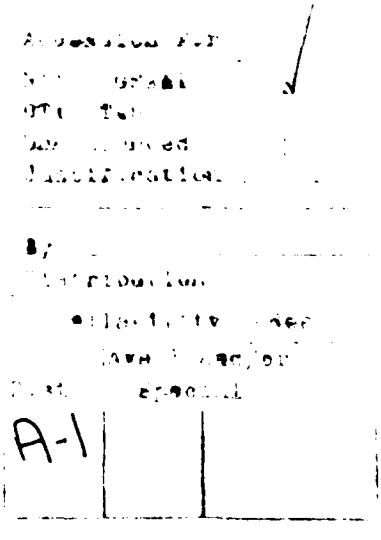

OFFICE OF NAVAL RESEARCH

ANNUAL TECHNICAL REPORT

for

October 1, 1990 through September 30, 1991

for

Contract N00014-87-K-0243

R&T #414e340

Materials Processing of Diamond: Etching, Doping by Ion Implantation and Contact Formation

Max L. Swanson
University of North Carolina
Department of Physics and Astronomy
CB#3255 Phillips Hall
Chapel Hill, NC 27599-3255

1. OVERVIEW

Three main areas of research were pursued in this period. The first was a continued study of the ion implantation doping of natural diamond, using dual implantations of C plus B. Of special concern was the measurement of resistance versus temperature using four point probes, to avoid edge effects and contact resistance. The result of these measurements was in general the elimination of the low activation energies occurring at the low temperature end of the resistance/temperature plot, which were apparently due to small edge resistances.

The second area was the attempt to dope natural diamond n-type by implantation with Na and Li, in collaboration with Oak Ridge National Laboratories. Linear Arrhenius plots of logR vs 1/T were obtained, with an activation energy of near 0.4 eV. However, the resistivity was high, and it increased on annealing, indicating possible effects of radiation damage. The ultimate goal of this work is the diffusion of the dopant beyond the damaged region, followed by removal of the damage by plasma etching.

The third area was growth of heteroepitaxial diamond films on Cu substrates, using ion implantation of C. Both low temperature implantations followed by furnace or laser annealing in different ambients, and high temperature implantations were attempted, with the collaboration of Oak Ridge National Laboratories and the Research Triangle Institute. So far, the growth of diamond by this method has not been successful.

2. RESULTS

2.1 Dual Implantations with C plus B

Natural diamond was implanted with C and B at 77K, followed by furnace and rapid thermal anneals. Measurements were made of optical absorption, RBS/channeling and resistance/temperature. Attempts were also made to measure Hall effect, but in general the carrier concentrations were too small for meaningful results. Earlier resistance results used two point probes, with the contacts located on the sample edges. There are two disadvantages of this procedure: contact resistance and a possible low edge resistance. We have overcome these difficulties by placing four contacts away from the edges (using a masking method), and making the contacts via high dose B implantations. These contacts were metallic-like, so that W point probes could be utilized.

Some typical resistance/temperature curves are shown in Figs. 1(a) and 1(b). It is seen that the logR vs 1/T plots were almost linear, in contrast to many results in the literature, which exhibited strong curvature, especially at the lower temperature end. We attribute this curvature to edge resistance effects. In Fig 1(a), the curvature seen at the high temperature end was also present before implantation, and is suggestive of a nitrogen donor level.

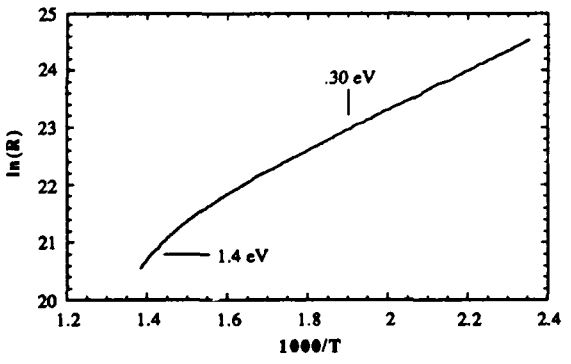

Fig. 1a: Arrhenius plot of R(T) for type IIa diamond co-implanted with carbon plus 5 x 10^{19}/cm^3 boron followed by RTA at 950°C.

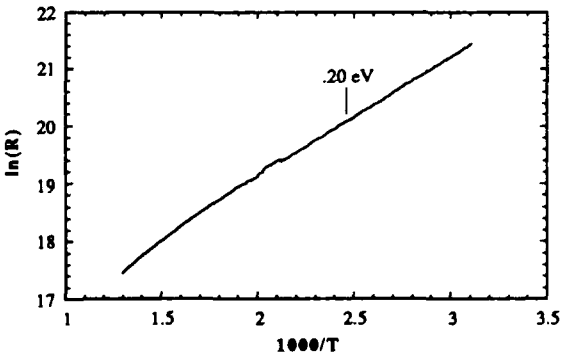

Fig. 1b: Arrhenius plot of R(T) as in Fig.1a but with a higher boron dose (1.5 x10^{20}/cm^3).

2.2 Implantation for n-type diamond

Motivation

Diamond is a wide band gap semiconductor/insulator. It has been known for some time that naturally occurring substitutional boron impurity results in a shallow acceptor level approximately 0.37 eV above the valence band. We have previously reproduced this effect by implanting boron into nominally pure single crystal diamond samples. In the present work we are studying the effects of other implanted impurities on the electronic levels.

Theoretical calculations predict that lithium and sodium should be interstitial donors in a diamond lattice with donor levels around 0.1 eV and 0.3 eV respectively.[1] Successful doping of lithium into single crystal diamond has been reported, but the fact that implantation damage also gives n-type behavior introduces doubt.[2,3] The conduction behavior due to the lithium implantation disappeared after thermal annealing. This could be a result of either lithium diffusion or damage recovery. An advantage of sodium doping would be less diffusion.

Procedure and Results

Sodium was implanted into type IIa single crystal diamonds. The implantations were done using several different incident energies in order to produce a wide uniformly doped layer (Figs. 2a and 2b). Total dopant concentration was limited by the amount of implantation damage which could be recovered by thermal annealing. This limit has been determined in previous studies.

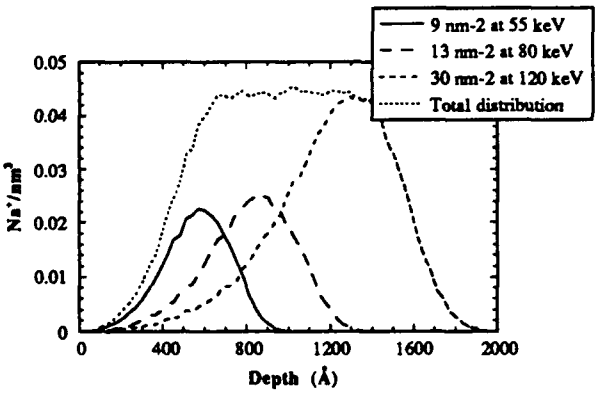

Figure 2a: Implanted sodium ion distribution simulated by TRIM.

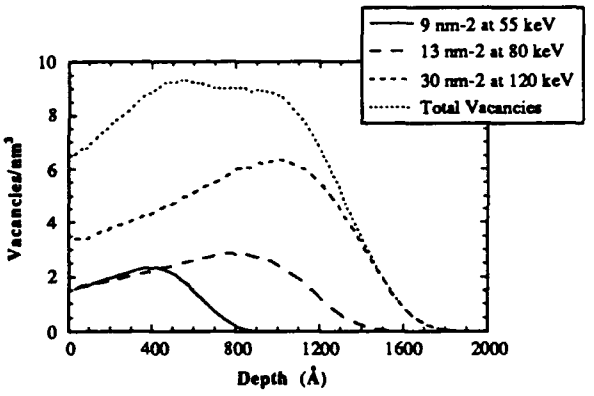

Figure 2b: Vacancy distribution resulting from sodium implantation (TRIM simulation).

Contact to the implanted layer was achieved by high dose implantation of boron at the edge of the implanted region. The effect of this implantation is the amorphization of the diamond to a certain depth controlled by the implant energy. After thermal annealing and chemical removal of graphite with chromic acid, the diamond is etched down to the doped layer and a highly conductive spot is left as a contact. Ohmic contact can be achieved by placing tungsten probes on these spots.
The implanted layer is electrically isolated by the surrounding unimplanted region of the diamond. The resistance between two contacts on an unimplanted crystal is typically several orders of magnitude greater than after implantation.

The activation of free carriers from a bound level in diamond has been estimated by most authors by equation (1a). In this case electrons (n ≡ free electron concentration) are activated from an impurity donor level E_D below the conduction band minimum.

$$\frac{n(n+N_A)}{N_D-N_A-n} = \left(\frac{2\pi m^* kT}{h^2}\right)^{3/2} \exp(-E_D/kT) \qquad (1a)$$

This equation takes into account the concentration of donors (N_D) and the concentration of compensating acceptors (N_A). The free electron concentration can be measured through the Hall coefficient (R) by

$$n = (\mu_H/\mu_C)/eR, \qquad (1b)$$

where the mobility ratio μ_H/μ_C is often taken as $3\pi/8$. Equation (1a) is useful in two temperature ranges.For $T\rightarrow\infty$, which for diamond is effectively 1250 °C, n tends to N_D-N_A. For temperatures much less than 1250 °C, n « N_D or N_A and eq. (1a) reduces to

$$n \propto T^{3/2}\exp(-E_D/kT). \qquad (1c)$$

A plot of k(ln(n)-3/2lnT) vs. 1/T should therefore be a straight line of slope E_D.

The ionization energy for electrons bound by a donor level E_D below the conduction band minimum can also be estimated from temperature dependent conductance measurements. The conductivity is related to the free electron concentration by

$$\sigma = ne\mu_c. \qquad (1d)$$

From equation (1c) we have

$$\sigma \propto \exp(-E_D/kT), \qquad (1e)$$

if the temperature dependence of μ_c goes as $T^{-3/2}$. In fact, μ_c has been measured to have approximately this temperature dependence, and since the exponential function dominates the temperature dependence in σ, this approximation is reasonable.[4]

The resistance of the sodium-implanted layer between two contacts (away from the edges) was measured as a function of temperature (Fig. 3a). The data were analyzed by fitting to the above conduction theory. Plots of ln(R) vs 1000/T from 50 °C to 500 °C show a linear behavior which supports the theory. The slope of these curves give E_D/k and the y-intercept of the extrapolated line gives what shall be called R(∞), which should be related to the total donor concentration. The initial measurement also served as a 500 °C anneal, which resulted in a change in both the optical and electrical characteristics of the sample. Further annealing to 1100 °C for 10 seconds resulted in a continuation of this trend (figs.3a and 3b). These results were repeated on a second sample.

Optical absorption was used as a qualitative measure of the damage in each sample. Vacancies created by ion implantation result in optical absorption in the UV-visible spectrum above the 223 nm bandgap (Fig. 3b). Increase in the percent transmission in this range represents a decrease in the vacancy density, probably due to vacancy-interstitial recombination.

SIMS analysis was performed on several implanted samples. The SIMS profiles of the diamonds implanted below 50 °C agreed with the expected dopant distribution as determined by TRIM simulation (fig. 1a). Analysis of implantations performed at elevated temperatures will be obtained soon. After performing the thermal anneals described below, no measurable diffusion was discerned.

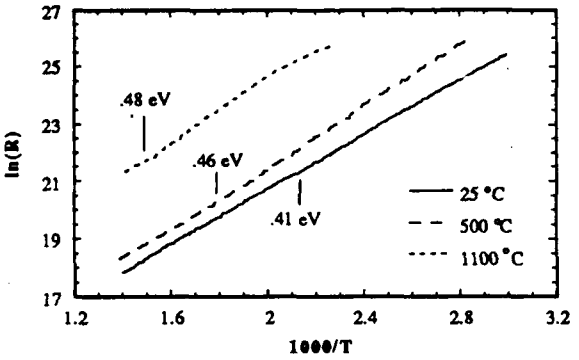

Figure 3a: Arrhenius plots of R(T) showing activation energy of conduction mechanism for Na^+ implanted at 77 K followed by annealing.

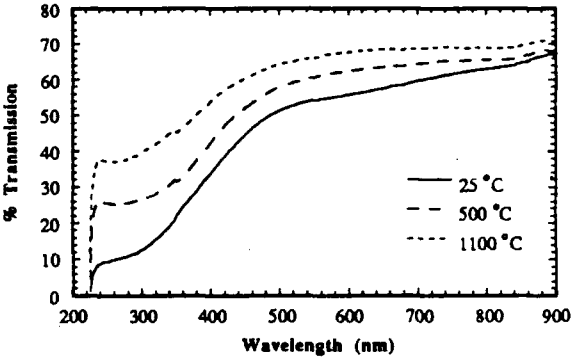

Figure 3b: Optical transmission through sample in fig. 3a after various anneals.

Sample B was implanted at 25 °C. The initial electrical behavior was similar to the samples implanted at low temperature. A 30 minute anneal at 950 °C resulted in a degradation of the sample conductivity; an activation energy was determined from 350 °C to 500 °C.

Sample C was implanted at 550 °C and then cooled to room temperature. This sample exhibited a single conduction mechanism with a well defined activation energy, 0.415 eV, from 50 to 500 °C (fig. 4a). There was no effect on the electrical behavior due to further annealing at 500 °C.

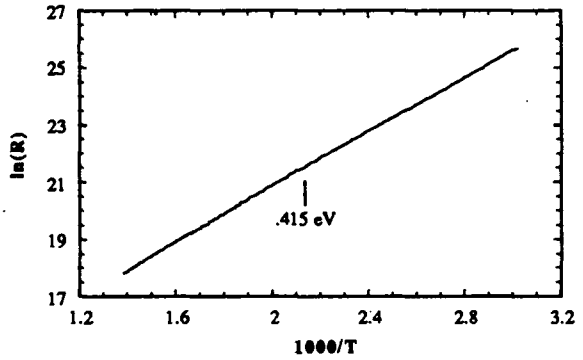

Figure 4a: Sample C: Arrhenius plot of R(T) showing activation energy of conduction mechanism for Na^+ implantation at 550 °C.

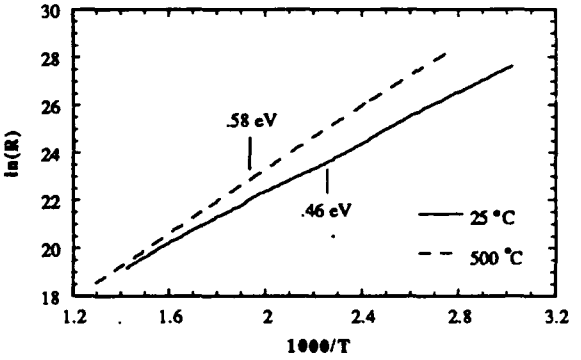

Figure 4b: Sample E: Arrhenius plot of R(T) showing activation energy of conduction mechanism for Ne^+ implantation at 77 K.

Sample D was implanted at 910 °C and then cooled to room temperature. This sample showed the least amount of optical absorption. The resistance was so high that ohmic contact could not be achieved at room temperature. An activation energy was obtained above 365 °C. The results of the Na implants are summarized in Table 1.

In order to isolate the effect of implantation damage on the conduction, sample E was implanted with neon 22 at 77 K. Neon, having all filled orbitals should not act as an electron donor as is expected in the case of sodium with its one loosely bound electron. On the other hand, neon 22 and sodium 23, being nearly the same mass, should create the same implantation damage profile under identical implant conditions. The neon implanted sample exhibited similar electrical characteristics to those observed for the sodium implants (fig. 4b).

Table 1: E_D and R(Ω) as a function of implant and anneal temperature.

Na^+ Implant Temperature	Anneal Temperature			
	25 °C	500 °C	1000 °C	950 °C
-196 °C	.41 eV, 73 kΩ	.46 eV, 49 kΩ	.48 eV, 729 kΩ	
-196 °C	.40 eV, 109 kΩ	.48 eV, 36 kΩ		
25 °C	.43 eV, 53 kΩ	.45 eV, 48 kΩ		.64 eV, 294 kΩ
550 °C	.415 eV, 73 kΩ	.415 eV, 73 kΩ		
910 °C	.66 eV, 104 kΩ			
-196 °C (Ne^+)	.46 eV, 133 kΩ	.58 eV, 20 kΩ		

Discussion

The electrical resistance measurements support the model of a single impurity level being introduced by implantation of sodium into natural diamond. The diamond is expected to be n-type but the high resistance of the implanted layer in conjunction with a low Hall mobility has made Hall effect measurements impossible at this time. A high temperature Hall effect system is being designed with the hope of decreasing the noise associated with high impedance samples.

Thermal annealing has produced two measurable effects that may be related. Optical measurements shows a decrease in the optical absorption of the implanted layer after annealing. It has been observed by RBS/channeling that this effect is associated with a recombination of vacancy/interstitial pairs in the damaged region. Electrically we see that R(∞) increases after the 950 °C and 1100 °C anneals; this shows a decrease in the number of donor centers. With the fact that no sodium diffusion was seen in the SIMS measurement, this suggests that the damage is somehow responsible for the conduction mechanism. This conclusion is supported by the fact that neon 22, which should not contribute any free electrons, produced similar results when implanted under identical conditions. Previous results however, both of our own research and work by other groups, found ion implantation damage to give a much lower activation energy (typically E_D<0.1eV).

Lower temperature implantations showed a slight change in the electrical behavior after a 500 °C anneal. The 500 °C anneal also resulted in some damage recovery. The slight decrease in R(∞) may be misleading in that the slope of the lines increased slightly and the extrapolation of this line to zero is only a rough analysis of the donor concentration.It should be noted that the samples never exhibited a decrease in resistance due to thermal annealing.

It has been mentioned that the implantation dose is effectively limited by the amount of implantation damage that can be recovered by thermal annealing. Higher temperature implantation allowed introduction of the dopant with less damage accompaniment. This effect allows implantation to a higher dopant concentration. The dopant amount can also be increased by iterative steps of implantation followed by annealing.

The implant temperature also had an effect on the electrical characteristics of the doped layer. Implantation at 550 °C resulted in the same type of electrical behavior as was observed in the lower temperature implants but proved stable to annealing at 500 °C. Implantation at 910 °C yielded a result different from the lower temperature implants. The layer's high resistance at room temperature prevented obtaining ohmic contact so the conduction mechanism at lower temperature could not be investigated. Above 365 °C, ohmic contact was achieved and an activation energy was measured similar to that observed at high temperature for the sample implanted at room temperature and annealed to 950 °C.

2.3 Heteroepitaxial growth of diamond

A novel ion beam method for growth of diamond on Cu crystals has been reported by Prins and Gaigher[5] and by Narayan et al. [6]. This method consists basically of implanting C into a material that has a very low solubility for C but a good lattice match to diamond. If the implantation is done at high temperatures where the implanted C atoms are mobile, the Cu lattice will reject the C atoms, resulting in diffusion of the C to the surface and formation of an epitaxial diamond film. Success in this method has been reported by Prins and Gaigher[5], who implanted C into Cu at elevated temperatures (up to 900°C), and a patent has been issued. However, up to now single crystal diamond has not been formed on single crystal samples of Cu by this method. It appears that the preparation of the Cu surface is very important in such experiments, since the presence of a very small amount of graphitic carbon on the Cu surface will cause nucleation of graphite rather than diamond. A similar method was reported by Narayan et al.[6], whereby the C ions were implanted into single crystalline Cu at room temperature, and the Cu was subsequently excimer laser-annealed to achieve monocrystalline films of diamond of about 50 nm thickness. Difficulties in reproducing these latter results are probably related to the critical laser pulse energy and duration, and to the fact that the diamond is buried near the Cu surface, so that delicate etching is required to reveal it. Similar experiments have been performed using Ni substrates, but in the case of Ni, carbide formation occurs, which is clearly detrimental.

We have implanted single crystalline and polycrystalline Cu with C ions (at MCNC and ORNL) at both low and high temperatures, in vacuum or under H ambient. The samples that were implanted at low temperatures were annealed in UHV or under H gas, and excimer laser annealing was also performed. Characterization of the samples was by microscopy, XPS, RBS/channeling and Raman scattering. Although different features on the Cu surface were observed, and it was clearly shown that the C had diffused to the surface, no evidence for diamond nucleation has so far been seen.

An example of XPS data for a Cu(100) crystal after implantation at 293K with 10^{18} C ions/cm^2 at 125 keV, followed by annealing, is given in Fig. 5. The data show that after annealing at 890°C for 1 h in UHV, a strong Cu Auger signal was present, as well as a C signal, indicating that only a thin layer of C atoms had diffused to the surface. However, after annealing for 1 h at 908°C, the Cu signal had almost disappeared, and the C line was stronger, indicating that the C surface layer was sufficiently thick to block the Cu signal. Scanning electron microscopy images of the sample after this anneal showed a network structure of carbon on the surface (Fig.6). Raman spectra showed no evidence of the characteristic 1332 cm^{-1} diamond line in these samples.

For samples implanted hot in hydrogen gas, similar data were obtained. The Raman spectra indicated microcrystalline graphite, as shown in Fig. 7. The strong signals seen at 1350 cm^{-1} and 1590 cm^{-1} have been observed previously for CVD diamond-like layers[7]. It should be noted that the Raman cross section for graphite at 1580-1590 cm^{-1} is about 50 times larger than that for diamond at 1332 cm^{-1}, so that it is difficult to observe a small fraction of diamond in a graphite layer.

These results show that the C implantation of Cu samples at low temperature, followed by annealing, or C implantation at elevated temperatures does produce a diamond-like layer of C on the surface, but that the critical conditions for monocrystalline diamond growth were not achieved.

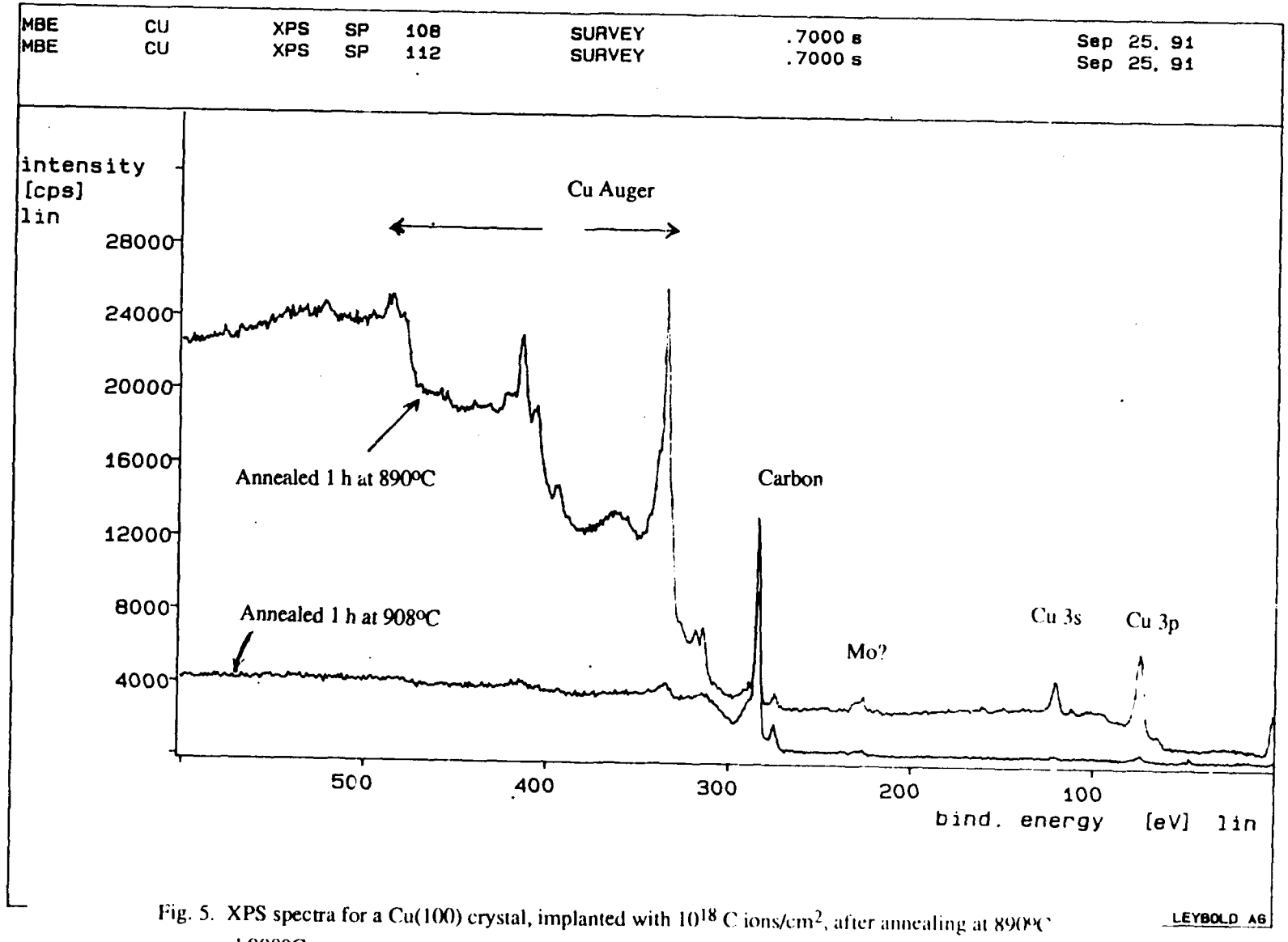

Fig. 5. XPS spectra for a Cu(100) crystal, implanted with 10^{18} C ions/cm^2, after annealing at 890°C and 908°C.

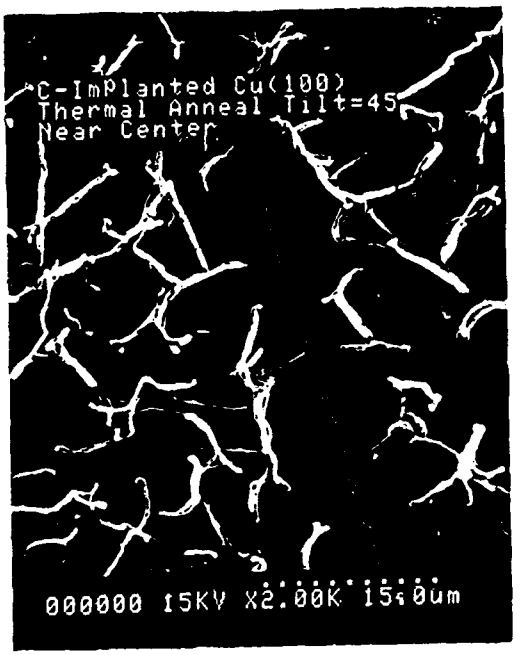

Fig. 6. Scanning electron micrograph of the Cu(100) crystal of Fig. 5 after the 908°C anneal.

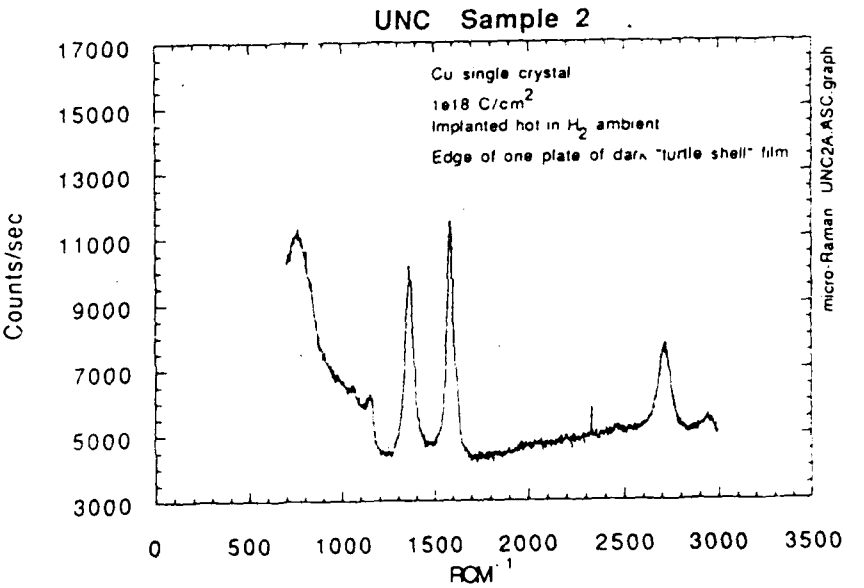

Fig. 7. Raman spectrum of a Cu single crystal after implantation with C to 10^{18} ions/cm^2 in H_2 gas at 900°C.

REFERENCES

1. J. Bernholc, S.A. Kajihara, and A. Antonelli, in "New Diamond Science and Technology", eds. R. Messier et al. (MRS Pittsburgh, 1991), p. 923.
2. V.S. Vavilov et al., Sov. Phys. Semicond. **13**, 604 (1979); **13**, 635 (1979).
3. G. Braunstein and R. Kalish, Appl. Phys. Lett. **38**, 416 (1981).
4. A.G. Redfield, Phys. Rev. **94**, 526 (1954).
5. J.F. Prins and H.L. Gaigher, in "New Diamond Science and Technology", eds. R. Messier et al. (MRS, Pittsburgh, 1991), p.561.
6. J. Narayan, V.P. Godbole and C.W. White, Science **252**, 416 (1991).
7. R.J. Nemanich, J.T. Glass, G. Lucovsky and R.E. Shroder, J. Vac. Sci. Technol. **A6**, 1783 (1988).

Annual Technical Reports Distribution List

SDIO/IST Crystalline Carbon Materials Program

(to be incorporated into report as its final pages

addressee	quantity
1. ONR Arlington, VA 22217 ATTN: Code 1114 Code 1131M	6 1
2. Defense Documentation Center Bldg. 5 Cameron Station Alexandria, VA 22314	12
3. Naval Research Laboratory Washington, DC 20375 ATTN: Code 4683 Code 2627 Code 6820 Code 6211 Code 6684 Code 6115 Code 4684 Code 6174	1 6 1 1 1 1 1
4. Naval Ocean Systems Center San Diego, CA 92152 ATTN: Code 1211 Code 911 Code 56	1 1 1
5. (Cognizant ONR Resident Representative or DCASMR)	1
6. SDIO/IST Pentagon Washington, DC 20301-7100	1
7. DARPA/D.S.O. 1400 Wilson Blvd. Arlington, VA 22209	1

addressee	quantity
8. Dr. M. Geis M.I.T. Lincoln Labs Lexington, MA 02173-0073	1
9. Prof. R. Messier 265 Materials Res. Lab. University Park, PA 16802	1
10. Prof. R. Davis Materials Eng., N.C.S.U. Raleigh, NC 27695-7907	1
11. R. Markunas R.T. Instit., P.O. Box ~~[illegible]~~ R.T. Park, NC 27709-2194	1
12. Prof. G. Walrafen Howard Univ., Chemistry Dept. 5325 Potomac Ave., N.W. Washington, DC 20016	1
13. Prof. I. Lindau Synchrotron Radiation Lab. Stanford, CA 94305	1
14. A. J. Purdes M.S. 147 Texas Instruments, P.O. Box 655936 Dallas, TX 75265	1
15. W. D. Partlow Westinghouse R&D Ctr 1310 Beulah Road Pittsburgh, PA 15235	1
16. R. L. Adams 21002 N. 19th Ave., Suite 5 Phoenix, AZ 85027	1

Annual Technical Reports Distribution List

SDIO/IST Crystalline Carbon Materials Program

(to be incorporated into report as its final pages)

addressee	quantity
17. Prof. J. Angus --Dept. of Chemistry Case Western Reserve Univ. Cleveland, OH 44106	1
18. T.R. Anthony, GE R&D Bldg. K-1, Room 1C30 Schnectady, NY 12345	1
19. Yehuda Arie SRI Sarnoff Center Princeton, NJ 08540	1
20. P.J. Boudreaux, Lab for Phys. Sci. 4928 College Avenue College Park, MD 20740	1
21. Prof. R.F. Bunshaw, UCLA 6532 Boelter Hall Los Angeles, CA 90024	1
22. Ray Calloway, Aerospace Corp. P.O. Box 92957 Los Angeles, CA 90009	1
23. Prof. M.L. Swanson Phillips Hall CB # 3255 Chapel Hill, NC 27599-3255	1
24. IBM T.J. Watson Center Yorktown Heights, NY 1059 8 ATTN: J.J. Cuomo B. Meyerson	1 1
25. Prof. J. L. Davidson 200 Broun Hall Auburn Univ., AL 36849	1
26. Prof. P.H. Fang, Dept. of Physics Boston College Chestnut Hill, MA 02167	1

addressee	quantity
27. Wen Hsu, Div 8347 Box 969 Sandia National Labs Livermore, CA 94550	1
28. Prof. W. Lanford Physics Dept. S.U.N.Y. Albany, NY 12222	1
29. Prof. E.S. Machlin 44 Morningstar Drive Croton-on-Hudson, NY 10520	1
30. Prof. J. Mayer 210 Bard Hall Cornell University Ithaca, NY 14853	1
31. Prof. J. Pancove, ECE Univ. of Colorado Boulder, CO 80309-0425	1
32. Michael Pinneo, Crystallume 3180 Porter Drive, Suite 2 Palo Alto, CA 94304	1
33. Kenneth Russell J.P.L. M.S. 122-123 4800 Oak Grove Drive Pasadena, CA 91109	1
34. Prof. T. D. Moustakas Exxon Research Annandale, NJ 08801	1

Encl. (2)